

# Industrial Energy Disaggregation with Digital Twin-generated Dataset and Efficient Data Augmentation

Christian Internò<sup>\*†</sup>, Andrea Castellani<sup>†</sup>, Sebastian Schmitt<sup>†</sup>, Fabio Stella<sup>‡</sup>, and Barbara Hammer<sup>\*</sup>

**Abstract**—Industrial Non-Intrusive Load Monitoring (NILM) is limited by the scarcity of high-quality datasets and the complex variability of industrial energy consumption patterns. To address data scarcity and privacy issues, we introduce the Synthetic Industrial Dataset for Energy Disaggregation (SIDED), an open-source dataset generated using Digital Twin simulations. SIDED includes three types of industrial facilities across three different geographic locations, capturing diverse appliance behaviors, weather conditions, and load profiles. We also propose the Appliance-Modulated Data Augmentation (AMDA) method, a computationally efficient technique that enhances NILM model generalization by intelligently scaling appliance power contributions based on their relative impact. We show in experiments that NILM models trained with AMDA-augmented data significantly improve the disaggregation of energy consumption of complex industrial appliances like combined heat and power systems. Specifically, in our out-of-sample scenarios, models trained with AMDA achieved a Normalized Disaggregation Error of 0.093, outperforming models trained without data augmentation (0.451) and those trained with random data augmentation (0.290). Data distribution analyses confirm that AMDA effectively aligns training and test data distributions, enhancing model generalization. The dataset SIDED and related code is publicly available at <https://github.com/ChristianInternò/SIDED>.

**Index Terms**—Non-Intrusive Load Monitoring, Energy Disaggregation, Deep Learning, Data Augmentation, Digital Twin, Industrial Data

## I. INTRODUCTION

**E**NERGY management has become increasingly important due to the undeniable reality of climate change and the rising global energy demand [1]. The industrial sector plays a significant role in international energy optimization [2], [3], necessitating heightened awareness of energy consumption to enhance efficiency and sustainability.

Non-Intrusive Load Monitoring (NILM) [4] enables monitoring of individual appliance energy consumption without installing dedicated sensors, by analyzing measurements from the main power meter. This approach avoids the impracticality

and expense of widespread sensor deployment [5] and enhances the accuracy of energy management systems [6].

While machine learning-based NILM methods have achieved results on residential datasets, where appliances generally exhibit discrete on/off behavior and low variability [7], [8], these methods struggle in industrial environments. Industrial facilities include a greater variance and magnitude of power signals, with continuously varying, non-linear power profiles from Variable Frequency Drives (VFDs) and Constantly-on Variable Appliances (CVAs), along with integrated energy-producing systems. In addition, the scarcity of publicly available industrial datasets, exacerbated by privacy and security issues [9]–[12], further complicates model development and generalization for industrial applications.

While recent work has explored the use of Digital Twin technology to simulate industrial energy data [13]–[17], no comprehensive and fully accessible industrial NILM dataset has been produced that captures the full complexity of industrial loads. Moreover, conventional data augmentation (DA) techniques—designed primarily for residential data, are not suited to address the continuous overlapping nature of industrial signals and do not account for the wide variance in appliance power levels.

In order to bridge these research gaps, our contributions are twofold:

1) SIDED, a novel Digital Twin-generated Synthetic Industrial Dataset for Energy Disaggregation. SIDED encompasses three types of industrial facility configurations across three geographic locations (Los Angeles, Tokyo, and Offenbach), capturing diverse appliance behaviors, weather conditions, and load profiles to provide a rich benchmark for industrial NILM research. SIDED leverages Digital Twin technology carefully calibrated on real operational data [18], which is uniquely tailored to capture the intricate dynamics, heterogeneity, and non-stationarity of industrial energy consumption.

2) Appliance-Modulated Data Augmentation (AMDA), specifically designed to handle the continuous and overlapping nature of industrial energy signals. AMDA is designed to enrich the training dataset with context-specific data points by analyzing the incidence and power levels of each appliance within an industrial building. Other DA techniques [19], such as rotation, translation, cropping, flipping, or mixing do not adequately cover the variance in power magnitudes, which is critical for enhancing the generalization of industrial NILM systems due to the strong presence of CVA and VFD appliances. Our method significantly enhances the training data, facilitating the

<sup>\*</sup> C. Internò and B. Hammer are with the Machine Learning Group, Center for Cognitive Interaction Technology (CITEC), University of Bielefeld, Bielefeld, Germany.

<sup>†</sup> C. Internò, A. Castellani and S. Schmitt are with the Honda Research Institute EU, Offenbach am Main, Germany.

<sup>‡</sup> F. Stella is with the Models and Algorithms for Data and Text Mining Laboratory (MADLab), Department of Informatics, Systems and Communication (DISCo), University of Milano - Bicocca, Milan, Italy.

Christian Internò and Andrea Castellani contributed equally to this work. This work has been submitted to the IEEE for possible publication. Copyright may be transferred without notice, after which this version may no longer be accessible.

effective training of NILM models in a targeted, non-random manner. AMDA is particularly efficient in resource-constrained NILM environments, thanks to its modulated augmentation strategy.

We validate the effectiveness of AMDA through two industrial NILM evaluations using the SIDED dataset and state-of-the-art models. The first evaluation investigates the system’s adaptability to appliance-level changes, such as reconfiguration or removal. The second focuses on the model’s generalization across different facility setups, characterized by varying weather conditions and load profiles. Additionally, we analyze how AMDA improves the alignment between training and test data distributions. Together, these evaluations demonstrate AMDA’s ability to effectively bridge distribution gaps in industrial NILM scenarios.

The rest of the paper is structured as follows: in Section II, we review related works in NILM, highlighting the gaps in the current literature. Section III outlines the general NILM problem and provides a comparative analysis of industrial versus residential NILM techniques, illustrating how different load characteristics necessitate distinct models. In Section IV, we introduce the SIDED dataset and detail the proposed Appliance-Modulated Data Augmentation (AMDA) approach. In Section V, we outline the experimental setup used in our work, then Section VI presents quantitative results on both appliance variation and facility variation scenarios. Finally, Section VII concludes the paper and discusses future directions.

## II. RELATED WORK

Over the past decade, traditional NILM techniques such as Factorial Hidden Markov Models and Combinatorial Optimization [20] have shown effectiveness in settings where appliances switch between discrete on/off states, making them suitable for many residential contexts. However, these methods struggle in industrial scenarios where VFD and CVA devices exhibit smooth and overlapping power signals [10], [12]. Such continuous load variations require more flexible models capable of handling non-linear dynamics.

Machine learning (ML) methods, including classical Support Vector Machines and Decision Trees [20], have been tried for NILM, but recent work favors Deep Neural Networks (DNNs) due to their capacity to capture complex dependencies and achieve superior disaggregation accuracy [7]. Despite these advantages, DNNs are data-intensive and demand substantial labeled data—often impractical in industrial environments marked by limited data availability, privacy concerns, and heterogeneous equipment [11].

Data scarcity in industrial NILM settings is compounded by the strict confidentiality requirements of industrial processes, the unique operational schedules of each facility, and generally higher power levels than those seen in residential contexts [4], [10], [12]. To address the lack of annotated data, researchers have proposed DA strategies adapted from time-series analysis, such as slicing, warping, and scaling [19]. However, these approaches must be applied cautiously to avoid introducing artifacts that misrepresent actual consumption behavior [12].

Moreover, many DA techniques have been tailored for residential appliances and do not directly generalize to continuously varying industrial loads [13], [17].

Another avenue for expanding training resources is the use of Generative Adversarial Networks (GANs) [21], which can synthesize realistic consumption patterns. GAN-based solutions, however, often require large amounts of pre-existing data and computational power [22], presenting further barriers in resource-constrained industrial settings.

Digital Twin technology has recently emerged as a promising tool for generating synthetic data that closely mirrors real-world industrial conditions, while maintaining privacy [16], [22], [23]. Although Digital Twins have been used for tasks like anomaly detection [15], smart grid optimization [24], and industrial IoT energy management [14], their application in producing comprehensive synthetic datasets for NILM remains limited. Much of the existing work centers on operational optimization rather than generating load signatures of multiple industrial devices. Additionally, there remains a gap in dedicated DA techniques specifically designed for the continuous and overlapping loads that dominate industrial energy profiles [12].

Existing industrial NILM datasets present limitations that underscore the need for a more comprehensive resource. For instance, the IMDELD [25] was acquired in a poultry feed factory, covering data over a relatively short duration of 111 days from a single geographic location. Similarly, the HIPE [26] was collected in an electronics manufacturing facility over approximately three months with a 5-second sampling interval. Although IMDELD and HIPE reflects certain aspects of manufacturing processes, their short recording period and confinement to a single location prevent it from representing seasonal variations and multi-site operational differences. Moreover, the LILACD [27] is derived from a controlled laboratory environment. The dataset does not capture the full range of temporal variability—such as seasonal variations, different load profile from different across multiple industrial facilities and locations.

Motivated by these gaps, we introduce SIDED, a novel open-source industrial dataset generated via Digital Twin simulations, encompassing diverse appliance types across multiple geographical locations and facility profiles. To further enhance data diversity without sacrificing realism, we propose Appliance-Modulated Data Augmentation (AMDA), a computationally efficient DA method that scales each appliance’s power consumption according to its relative load contribution. By preserving signal integrity, AMDA yields more representative training samples that significantly improve NILM performance in the complex industrial environment.

## III. COMPARATIVE ANALYSIS OF INDUSTRIAL VS. RESIDENTIAL NILM

NILM techniques in residential and industrial settings face very different challenges due to variations in load behavior, signal characteristics, and environmental influences. In residential settings, the power consumption is typically generated

by a limited number of appliances operating in clearly defined, discrete states. In contrast, industrial settings feature a broad dynamic range with continuously varying loads, overlapping operating periods, and even simultaneous energy production.

**Residential NILM** is generally based on the assumption that the aggregate power consumption,  $x(t)$ , can be decomposed into a finite sum of appliance signals that switch between a small number of well-defined states. Its mathematical problem formulation is as follows [28]:

$$x(t) = \sum_{i=1}^N a_i(t) \cdot P_i + \epsilon(t), \quad (1)$$

where  $x(t)$  is the aggregate power at time  $t$ ,  $a_i(t) \in \{0, 1\}$  (or drawn from another limited discrete set) represents the state of the  $i^{\text{th}}$  appliance (e.g., off or on),  $P_i$  is the nominal power consumption of the  $i^{\text{th}}$  appliance, and  $\epsilon(t)$  models measurement noise. Residential environments typically involve a few common appliance types that exhibit clear step changes corresponding to switching events. These power profiles are predominantly consumption-only and are characterized by piecewise constant or step-like behavior [29].

Instead, **Industrial NILM** faces a different scenario. The different loads operate over a continuous range and often exhibit overlapping and non-discrete patterns due to the complexity of industrial processes. Its mathematical model is similar to (1), but it must accommodate continuous variability and incorporate exogenous factors such as ambient temperature, production schedules, and operational conditions: [28], [30]:

$$x(t) = \sum_{i=1}^N f_i(\mathbf{u}(t), t) + \eta(t), \quad (2)$$

where  $f_i(\mathbf{u}(t), t)$  is a continuous function representing the power profile of the  $i^{\text{th}}$  load, potentially dependent on external variables  $\mathbf{u}(t)$  (e.g., weather, operational schedules),  $\eta(t)$  captures both measurement noise and unmodeled dynamics. Industrial systems not only exhibit much higher power levels, with devices such as VFDs and CVAs showing smooth, non-linear power variations, but also include energy production elements like Combined Heat and Power (CHP) units and photovoltaic systems (PV). This mixed nature of consumption and production leads to aggregate signals with both positive and negative values. Rapid process variations and external influences can cause power fluctuations on the order of 30–50% over short intervals [29], [31]. Moreover, high-quality industrial datasets are often scarce and require advanced pre-processing techniques (e.g., robust normalization, denoising, and augmentation) to deal with the inherent heterogeneity and non-stationarity of the signals.

Table I summarizes the major differences between residential and industrial NILM. Residential NILM approaches handle discrete, isolated appliance states but fail when applied to industrial settings. In industrial environments, multiple devices and processes are frequently active simultaneously. The resulting overlapping signals create complex aggregate profiles that cannot be neatly decomposed using simple step functions. Industrial power consumption is subject to external factors (e.g., ambient temperature, operational cycles) that

TABLE I: Key Differences Between Residential and Industrial NILM.

	Residential NILM	Industrial NILM
<b>Appliance States</b>	Discrete (e.g., off/on)	Continuous, multi-pattern
<b>Signal Range</b>	Lower power levels	Higher power levels; includes production
<b>Data Variability</b>	Limited	High variability with overlapping signals
<b>Temporal Dynamics</b>	Step-like changes	Smooth, continuous dynamics
<b>Noise Characteristics</b>	Primarily measurement noise	Includes operational variability and external influences

TABLE II: Parameters characterizing the different facility, which are shared by every location (Germany, US and Japan).

Description	Office	Dealer	Logistic
Yearly energy demand from the grid ( <i>MWh</i> )	1334	162	1689
EVSE yearly energy charging ( <i>MWh</i> )	32	33	32
PV power ( <i>W</i> ) per $m^2$	210	150	150
PV area ( $m^2$ )	2000	2000	10000
CS nominal power ( <i>kW</i> )	900	250	4000
CS Usage Per Year ( <i>h</i> )	300	300	500
CHP nominal power ( <i>kW</i> )	340	210	900
Yearly energy BA demand ( <i>MWh</i> )	2032	501	4341
BA Server power ( <i>kW</i> )	69	20	20
Use server cooling	No	No	Yes
Weekly workdays	5	6	7

have little or no impact in residential settings. Residential models do not account for these covariates. The magnitude and variability of industrial loads, which often include both very high consumption and production components, demand a modeling approach capable of handling a wide range of values and subtle dynamic variations.

#### IV. DATASET AND DATA AUGMENTATION APPROACH

##### A. Synthetic Industrial Dataset for Energy Disaggregation

The proposed Synthetic Industrial Dataset for Energy Disaggregation (SIDED) is freely available at <https://github.com/ChristianInterno/SIDED>, it is compatible with NILMTK [32], a popular open-source toolkit designed to facilitate the comparison and development of NILM algorithms.

The dataset contains simulation data for three different realistic industrial facility types: Dealer, Office, and Logistics. Each facility is defined by its installed appliances and their characteristic electricity consumption profiles. In addition to the facility types, each facility can be located in one of three different geographic locations: Offenbach (Germany), Los Angeles (USA), and Tokyo (Japan). Each location has different environmental conditions defined by the temperature profile and sun radiation, which affect how the photovoltaic, cooling, and heating systems are operated. Moreover, working hours and holidays differ between the locations, which manifests itself in different load profiles for each appliance.

The dataset is generated using a high-fidelity Digital Twin simulator created with a physical simulation library<sup>1</sup>. The simulation model is based on physical models for all the machinery (CHP, cooling, heating, ventilation...), incorporating the realistic controller modules as in the real devices. It models physical effects on the facility buildings, such as irradiation heating, heat diffusion, and energy dissipation in pipes. The electricity and heating/cooling demand is taken from real measurement data and adjusted to the facility size. The weather data are collected through a weather station installed in the three locations for the year 2020. The simulation was thoroughly calibrated against real world measurement data from an industrial facility for one specific configuration (Office in Offenbach, Germany) [18], [33], [34]. The accumulated discrepancy error over one year between simulation and real-world measurement for this calibrated configuration is below 3% [18]. Due to the fact that the simulator is based on physical models and realistic controller systems, we are guaranteed to produce realistic and physically consistent data also for the other non-calibrated configurations.

The parameters characterizing the three simulated facilities simulated are summarized in Table II. The yearly energy demand from the grid for the three building types varies significantly, with the Office requiring 1334 MWh, Dealer requiring 162 MWh, and the Logistic building requiring 1689MWh. Each facility in the dataset contains profiles for five different appliances: Electric Vehicle Supply Equipment (EVSE), Cooling Systems (CS), Photovoltaic (PV), Combined Heat and Power (CHP), and Background Appliances (BA), which sums up all smaller devices such as computers, various machinery, servers, or other household appliances. The EVSE, BA, and SC are consumers of electrical energy, while PV and CHP are producers. The CHP system uses natural gas to produce electricity and heating, and its efficiency is 35%. Important configuration aspects are the size of the IT components (server power), the presence and size of separate server cooling, the presence and size of stationary battery storage, or the working days per week.

An example week of SIDED is depicted in Fig. 1, it shows the three different geolocations (Offenbach, LA, and Tokyo) and the three configurations (Office, Logistic, and Dealer). It is possible to observe the different consumption behavior of the different types of appliances and note how the producers (PV and CHP) report a negative power value. Additionally, the ambient temperature variation throughout the week is displayed, highlighting its potential correlation with the load profile of certain appliances, e.g., the CHP, CS, and PV. The aggregate signal  $A_t$  is the sum of the other appliances:  $A_t = \sum_{i=1}^n x_{i,t}$  where  $x_{i,t}$  is the signal from the  $i^{th}$  appliance at time  $t$ , and  $n$  is the total number of appliances. This aggregated signal represents what is measured at the main electrical meter i.e., the power drawn from the grid.

Fig. 2 depicts the energy flow diagram for the Office configuration in Offenbach, showing the yearly energy overview. The facility has a total production of 998 MWh (from PV and

CHP) and a consumption of 2334 MWh, resulting in 1334 MWh drawn from the distribution grid (referred to as 'Grid in' in the diagram). It shows the energy yearly overview, with the total production of 998 MWh, and consumption of 2334 MWh, thus 1334 MWh drawn from the distribution grid.

The SIDED dataset consists of the time series of the appliances, and the environment variables for each of the three facilities of each type in each of the three geographic location, in total 9 different configurations. The time series of each configuration covers a complete year from January to December, and the measurement readings are taken at a one-minute interval (sampling rate of  $\frac{1}{60} Hz$ ). As a result, each of the nine simulated facility patterns contains 525,600 individual data points. For each configuration, the time series included are: ambient temperature ( $K$ ), diffuse sky radiation ( $W/m^2$ ) that the PV system obtains scattered by atmospheric constituents such as clouds and dust, direct radiation ( $W/m^2$ ) from the sun to the PV system, aggregate electric power ( $W$ ), EVSE electric power ( $W$ ), PV production power ( $W$ ), CS electric power ( $W$ ), CHP electric power ( $W$ ), BA electric power ( $W$ ). All power values refer to the real power of the appliance. The weather and radiation data are not used in this work, but they are included in the SIDED for completeness and future applications.

To justify the choice of configurations and simulated appliances in SIDED, we align with previous classifications of appliances as delineated in [9]. Specifically, SIDED includes both CVA and VFD appliances, which are prevalent in industrial settings and contribute significantly to energy consumption patterns. The SIDED dataset incorporates all the following six groups of industrial appliances, each reflecting unique patterns of energy consumption:

- **Constantly-on Variable Appliances:** Industrial appliances that are never off and always present energy consumption during time, such as the CHP.
- **Periodical:** Industrial appliances such as EVSE and PV show periodic behavior in energy consumption.
- **Seasonal:** Appliances such as PV, CHP, and CS show seasonal behavior in energy consumption, being influenced by the changing weather of the seasons.
- **Multi pattern:** Industrial appliances in the multi-pattern category offer multimodal operation with different patterns of energy and power consumption. In SIDED all five appliances can be grouped as multi-pattern.
- **Consumers:** Industrial appliances that actively consume energy, such as EVSE, CS, and BA.
- **Producers:** Industrial appliances that actively produce energy, such as PV and CHP.

By including these diverse appliance types across various facility configurations and geographic locations, SIDED provides a comprehensive dataset that reflects the complexities of industrial energy consumption. To the best of our knowledge, SIDED is the only industrial dataset that encompasses all these types of appliances, making it a valuable resource for advancing research in industrial NILM.

<sup>1</sup>[Online] <https://www.ea-energie.de/en/projects/green-city-for-simulationx-2/>

<https://www.ea-energie.de/en/projects/>

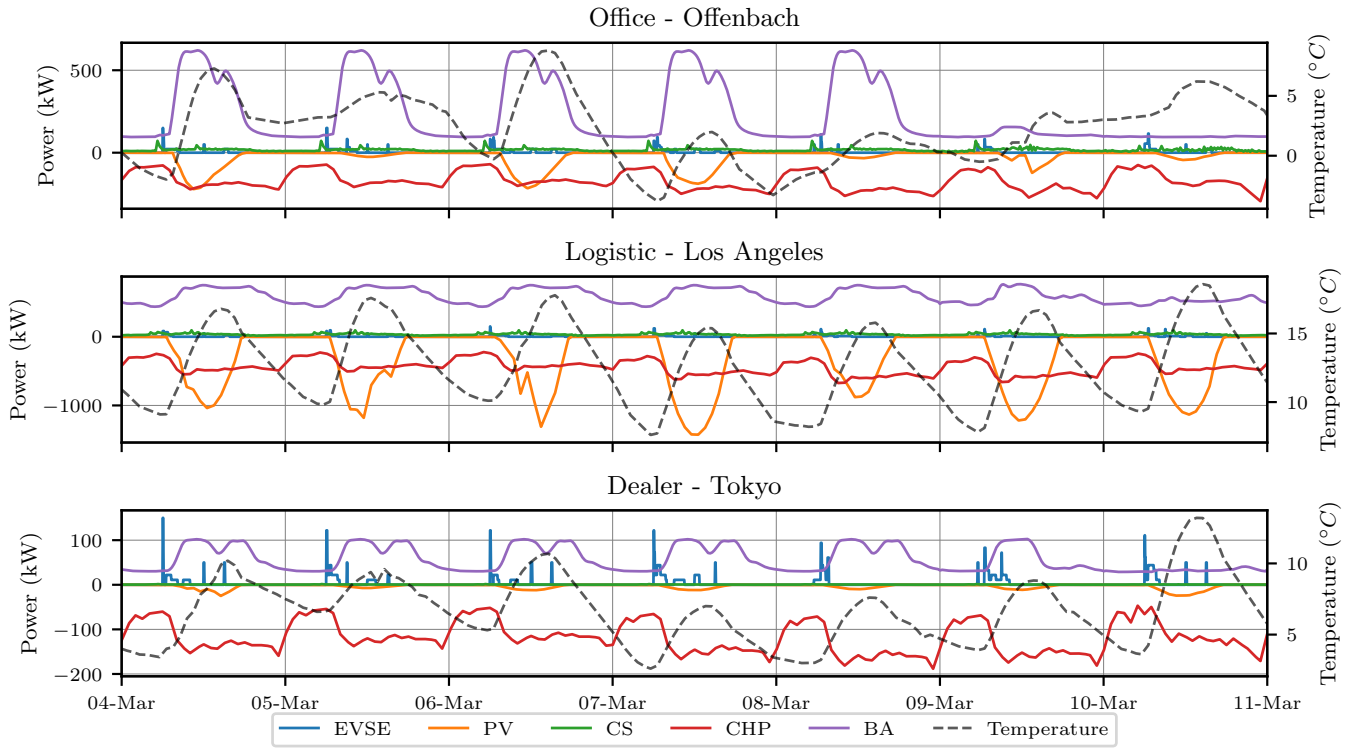


Fig. 1: Example week of SIDED with the different locations and configurations: Office in Offenbach (top) , Logistic in Los Angeles (center), Dealer in Tokyo (bottom). The different appliances are reported: Electric Vehicle Supply Equipment (EVSE), Cooling Systems (CS), Photovoltaic (PV), Combined Heat and Power (CHP), Background Appliances (BA), and ambient temperature. Negative values indicate power generation (PV, CHP).

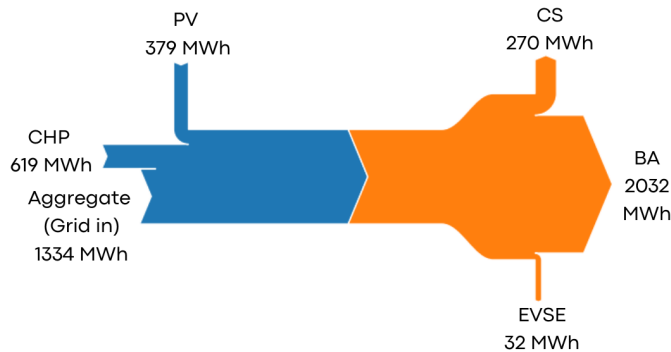


Fig. 2: Energy flow accumulated over one year with sources and consumers for the Office configuration in the Offenbach location.

### B. Appliance-Modulated Data Augmentation (AMDA)

Although the SIDED data set contains power signals for nine different facilities, totaling nine years of data, purely data-driven NILM approaches based on DNNs require more variations to generalize well to unseen configurations. Existing DA techniques often fail to capture the unique characteristics of industrial appliances with highly varying power magnitudes. To address this limitation, we introduce AMDA, a computationally efficient DA method designed to enhance the generalization capabilities of NILM models for industrial applications.

AMDA generates signals with greater variance in appliance power levels by scaling each appliance’s signal based on its relative contribution to the total power consumption. Instead of applying random scaling factors that may create unrealistic scenarios, we modulate the scaling factor  $S_i$  for each appliance  $i$  using its relative contribution  $p_i$ . The relative contribution  $p_i$  is defined as:

$$p_i = \frac{P_{\text{total},i}}{P_{\text{total}}}, \quad (3)$$

where  $P_{\text{total},i} = \sum_{t=1}^T |x_{i,t}|$  is the sum of the absolute values of the power consumed or produced by appliance  $i$ , and  $P_{\text{total}} = \sum_i P_{\text{total},i}$  is the total absolute consumption of all appliances.

In order to create additional data samples, AMDA re-scales each signal with an individual scaling factor  $S_i$ ,

$$\tilde{x}_{i,t} = S_i \cdot x_{i,t} \quad (4)$$

which is calculated as:

$$S_i = s \cdot (1 - p_i), \quad (5)$$

where  $s \geq 0$  is a hyper-parameter controlling the degree of augmentation. As a rule of thumb for tuning  $s$ , choose values that ensure the scaled signals remain within realistic operational limits for each appliance. For example, selecting  $s$  values between 1 and 5 allows for meaningful augmentation while respecting appropriate bounds. Within this range,  $s$  can be randomly selected to generate diverse augmented samples. Importantly, AMDA only modulates the relative magnitudes of

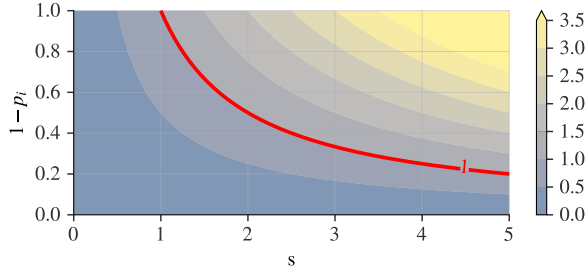


Fig. 3: Scaling factor  $S_i$  if Eq. (4) as a function of  $s$  and  $p_i$ . The red line indicates  $S_i = 1$ .

---

**Algorithm 1** Appliance-Modulated Data Augmentation (AMDA)
 

---

```

1: procedure AMDA(Dataset,  $s$ )
2:   for each appliance  $i$  in Dataset do
3:     Compute  $p_i \leftarrow \frac{P_{\text{total},i}}{P_{\text{total}}}$   $\triangleright$  Relative contribution
4:     Compute  $S_i \leftarrow s \cdot (1 - p_i)$   $\triangleright$  Scaling factor
5:     Scale signal  $\tilde{x}_{i,t} \leftarrow S_i \cdot x_{i,t}$ 
6:   end for
7:   Merge all  $\tilde{x}_{i,t}$  to form augmented aggregate signal
8:   Combine augmented signals with the original dataset
9: end procedure

```

---

individual appliance signals. It preserves the total aggregate power, ensuring that the overall profiles remain within realistic ranges, a critical property for industrial applications.

By scaling appliances based on their relative contributions, we amplify the representation of less significant appliances while reducing the impact of those with higher consumption. This ensures that no single appliance dominates the training data, allowing NILM models to learn more balanced patterns and improving their ability to generalize to new configurations.

For example, consider an appliance with a relative contribution  $p_i = 0.25$  and a chosen scaling parameter  $s = 1.5$ . The scaling factor becomes  $S_i = 1.5 \times (1 - 0.25) = 1.125$ , meaning the appliance’s signal is scaled up by 12.5%.

Figure 3 illustrates how  $S_i$  varies with different values of  $s$  and  $p_i$ . The red line represents  $S_i = 1$ , indicating no scaling. Values below the red line correspond to  $S_i < 1$ , where the appliance’s power is reduced. To generate one set of re-scaled data samples for augmentation, the procedure is applied to the series in the dataset with a fixed value of  $s$ . Algorithm 1 summarizes the AMDA method.

Table III presents the relative contributions  $p_i$  and total consumption  $P_{\text{total},i}$  for each appliance in different facility types located in Offenbach. Appliances like BA (Building Automation) have high  $p_i$ , resulting in lower scaling factors and reduced contributions in the augmented data. Conversely, appliances with lower  $p_i$ , such as PV and EVSE, receive higher scaling factors, enhancing their representation.

By generating new proportions between the contributions of each appliance, AMDA efficiently creates a training set with expanded and realistic variance, without relying on random modifications. This method maintains the temporal coherence of the signals and avoids introducing artifacts that could mislead the learning algorithms. It should be noted

TABLE III: Relative contributions  $p_i$  and total consumption  $P_{\text{total},i}$  (in kW) for each appliance in different facility types in Offenbach.

	Office		Dealer		Logistics	
	$p_i$	$P_{\text{total},i}$	$p_i$	$P_{\text{total},i}$	$p_i$	$P_{\text{total},i}$
EVSE	0.009	1,962	0.035	1,986	0.004	1,967
PV	0.114	22,800	0.041	2,303	0.181	92,626
CS	0.080	16,200	0.018	1,020	0.088	45,000
CHP	0.186	37,185	0.373	21,009	0.221	113,446
BA	0.601	121,921	0.533	30,076	0.507	260,497

that the computational demand of the AMDA method itself scales linearly with the amount of additional data generated. The operations to generate an additional data series are very efficiently implementable as they only consist of copy and rescale operations.

## V. EXPERIMENTAL SETUP

The code and data used in this work are publicly available at <https://github.com/ChristianInterno/SIDED>.

### A. Deep Learning Models

We conduct experiments with the deep neural network (DNN) architectures Long Short-Term Memory (LSTM) from [35], Temporal Convolutional Neural Network (TCN), and Attention-TCN (ATCN) from [36]. We employ the single-appliance NILM setting where the input is the aggregated power signal and the model extracts the power of a single appliance e.g., the CHP. In all of our experiments, we use the sequence-to-point network [37] structure: given a time series of aggregate power readings  $X = \{x_1, x_2, \dots, x_T\}$ , we use a sliding window of size  $w$  to create input sequences  $X_t = \{x_{t-w/2}, \dots, x_t, \dots, x_{t+w/2}\}$  for each time point  $t$  with  $t > w/2$  and  $t \leq T - w/2$ . The target output is  $y_t$ , the power reading of the appliance at time  $t$ . The DNN learns a function  $F$  mapping  $X_t$  to  $y_t$ :  $F(X_t; \theta) = y_t$ , where  $\theta$  represents the DNN parameters.

We use an LSTM network with three hidden layers, each containing 128 units. LSTMs are well-suited for capturing temporal dependencies in sequential data, making them effective for NILM tasks. The TCN model comprises eight layers that combine temporal convolutional and pooling operations. It has a receptive field covering the entire input sequence, allowing it to model long-range temporal patterns. The network processes single-channel input, produces 128 output channels, and incorporates batch normalization, ReLU activation, and a dropout rate of 0.33 to prevent overfitting. The ATCN [36] extends the TCN by introducing attention mechanisms. It generates multiple temporal residual blocks and uses attention to highlight the importance of each block for the target appliance, effectively capturing both long-term and short-term dependencies. All models are trained using the Adam optimizer with a learning rate of 0.001. We set the batch size to 64, employing early stopping based on validation loss to prevent overfitting.

### B. Data Preprocessing and Evaluation Metrics

For the current application, the one-minute resolution of the original data in the SIDED dataset is not necessary and we re-sample all time series to a sampling period of  $T_s = 5$  min in order to reduce the computation effort. Before feeding the data to any model, we normalize it for each building configuration with a RobustScaler [38], which normalizes data by subtracting the median and then scaling it according to the interquartile range. This ensures scaling is specific to each configuration, capturing the unique power distribution of appliances and avoiding inconsistencies from using a universal scaler across varying configurations.

Although our data is simulated, the signals in the SIDED dataset have varying power levels and can exhibit extreme values due to the dynamics of industrial appliances. We found that the RobustScaler effectively handles these variations and ensures that the model is not heavily influenced by extreme values. In order to be able to compare the results, all model outputs are de-normalized again in order to get time series signals on the original scales, and all performance metrics described below are calculated with de-normalized data.

We use sliding windows with a size of one day (288 samples at 5-minute intervals) and a stride of 25 minutes (5 samples). The window size is a hyper-parameter chosen to naturally reflect the daily characteristic behavior of the appliances, allowing the models to learn specific behaviors in the data.

As an example, Fig. 1 shows the usage cycles over a week of all signals for one Office Offenbach facility configuration. It highlights the periodic nature of device usage and the significant impact of working days on the BA signal. Additionally, the temperature varies throughout the week. This fluctuation may have a short-term correlation with the power consumption of specific appliances such as CHP, EVSE, and PV, and a long-term correlation with CS.

In the context of NILM, various metrics exist for evaluating results [9]. Since we are dealing with regression tasks and industrial appliances that are continuously on, rather than household appliances with on-off patterns, we employ regression-based evaluation metrics. Specifically, we use Mean Absolute Error (MAE), Mean Squared Error (MSE), the coefficient of determination ( $R^2$ ), and the Normalized Disaggregation Error (NDE) [39]. The NDE metric provides a dimensionless and normalized measure of disaggregation quality, facilitating fair comparisons across different appliances. These four metrics collectively offer a well-rounded evaluation of the complex and dynamic nature of industrial signals.

## VI. EXPERIMENTS AND RESULTS

We demonstrate the benefits of the proposed AMDA method in enhancing model generalization capabilities in realistic industrial settings with SIDED. We use quantitative metrics, distance measures and computational effort analysis to provide a comprehensive evaluation on:

**A. Appliance Variation Scenario:** We simulate a scenario where the power level of an appliance in the facility changes after the model has been trained. This experiment mimics real-world situations where new appliances are introduced, or existing ones are removed or reconfigured.

**B. Facility Variation Scenario:** We examine the performance of the NILM system when applied to a facility configuration different from the one used during training. This includes changes in geographic location, load profiles, and power levels for each appliance. We also compare training times and the computational effort required for AMDA.

**C. Data Distribution Alignment Analysis:** Finally, we quantitatively evaluate the information gained via AMDA, via KL and JS divergence to quantify the alignment between the distributions of the training and testing data. We use dimensionality reduction techniques like UMAP [40] to visualize the data distributions. This approach allows us to demonstrate how AMDA brings the training data distribution closer to that of the testing data, improving model performance.

In all experiments, we focus on single-appliance NILM, specifically targeting the disaggregation of the CHP appliance from the aggregate signal. We chose the CHP appliance due to its unique characteristics, including seasonality, susceptibility to weather variables, large fluctuations in machinery power, and its multi-pattern behavior. These factors make the CHP a challenging target for load disaggregation [6], [15]. The CHP system output not only vary in amplitude but also in their operating modes (e.g., duration, shape of transitions, and temporal dynamics) across different facilities due to their dependence on facility background load, demand and external temperatures. Due to the inclusion of different facility types and locations in our experimental setup (described below in Section VI-B) we can test the proposed augmentation algorithm in out-of-distribution scenarios, since the augmentation cannot natively adjust for different operating modes. For instance, by using an entirely unseen facility configuration (Logistics) during testing. The results indicate that, even under these conditions, models trained with AMDA outperform those trained with conventional augmentation methods.

To ensure a statistically robust evaluation of the models' performance, we repeat each experiment 20 times with different random seeds and model weight initializations. To assess the statistical significance of our results, we use the Critical Difference plot [41] to visualize and compare the performance of the models.

### A. Appliance Variation Scenario

In this experiment, we test how AMDA enhances the model's adaptability and generalization when there are changes in the consumption of a dominant appliance. We split our dataset into training, validation, and test sets with a random sampling of 72.25%, 12.75%, and 15% of the total Office Offenbach dataset, respectively. A unique aspect of our test set is the modification of the power level of the BA appliance, which plays a critical role in the aggregate signal by contributing over 60% of the total consumption (see Table III). While our model's input is the aggregate signal—the sum of all appliance power levels—individual appliances like the BA significantly influence this aggregate.

To create the modified test sets that simulate realistic scenarios where a major appliance undergoes changes (e.g., new appliances are introduced, or existing ones are modified

or removed), we modify the BA power level after the model has been trained. Specifically, we create modified test sets by multiplying the BA time series by the scaling factor  $s$ . Recall that this scaling factor is not part of the AMDA method; it is used solely to simulate changes in the BA appliance during testing. We vary  $s$  from 0 (completely removing the BA appliance) to 2 (doubling the BA appliance’s power level) in increments of 0.2. Note that  $s = 1$  corresponds to the default appliance setting, identical to the training set. All other appliances remain unchanged in the test sets.

We compare LSTM, TCN, and ATCN trained with and without AMDA. Using Algorithm 1 from Section IV-B, we generate the augmented training set with AMDA by applying two scaling hyper-parameters,  $s_1 = 1.5$  and  $s_2 = 4$ , to cover a larger variance. These  $s$  values are chosen arbitrarily to demonstrate the method’s effectiveness. For example, with  $s_1 = 1.5$ , since the BA appliance has a high relative contribution ( $p_{BA}$  is large), the modulated scaling factor computed as  $S_{BA} = s_1 \cdot (1 - p_{BA})$  results in  $S_{BA} = 0.598$  (see Fig. 3), which is less than 1, thus reducing its contribution. Conversely, for all other appliances with smaller relative contributions,  $S_i > 1$ , increasing their contributions. This occurs because the scaling factors are anti-correlated to the appliances’ relative contributions according to the AMDA method.

Table IV reports the results averaged over all the test sets. The inclusion of the AMDA method significantly improves the performance of all the DNN models, as indicated by a lower average rank compared to models trained without augmentation. The average rank is calculated by assigning ranks to each model for each performance metric and then averaging the ranks across all metrics. The best-performing model is the ATCN trained with AMDA, achieving average performance improvements of approximately 60% for MAE, 83% for MSE, 54% for  $R^2$ , and 81% for NDE compared to its counterpart trained without AMDA.

Figure 4 reports the results of the NDE metric for all test sets as a function of  $s$  applied to the BA appliance. The models trained with AMDA consistently outperform those trained without AMDA across all test scenarios. However, we observe a decrease in performance when the BA signal is reduced ( $s < 1$ ) during testing. This is likely because reducing the power of the BA appliance decreases the variance of the aggregate signal  $A_t$ , which heavily depends on BA’s contribution (see Table III). Lower variance in  $A_t$  makes the signal less informative, making it harder for the model to accurately disaggregate appliance-level consumption. In contrast, AMDA enhances training data by introducing varied operational scenarios, improving the model’s generalization and ability to generalize across different conditions.

### B. Facility Variation Scenario

We evaluate model generalization by training on data from the Office facility in Offenbach (80% training, 20% validation) and testing on the unseen data from the Logistics facility in Los Angeles. This scenario simulates the performance of a model in a facility with different operating conditions. We report results using the best-performing ATCN model from

TABLE IV: Average error metrics for experiment ‘Appliance Variation Scenario’. Asterisks (\*) indicate models trained with AMDA. The average rank is calculated by ranking each model based on its performance across all metrics.

	LSTM	TCN	ATCN	LSTM*	TCN*	ATCN*
MAE [MW]	0.033	0.033	0.029	0.015	0.013	<b>0.012</b>
	$\pm 0.012$	$\pm 0.008$	$\pm 0.012$	$\pm 0.008$	$\pm 0.009$	$\pm 0.008$
MSE [(MW) <sup>2</sup> ]	2.801	2.564	2.247	0.696	0.672	<b>0.476</b>
	$\pm 1.728$	$\pm 1.052$	$\pm 1.427$	$\pm 0.761$	$\pm 0.776$	$\pm 0.689$
$R^2$	0.490	0.540	0.596	0.879	0.880	<b>0.911</b>
	$\pm 0.318$	$\pm 0.183$	$\pm 0.254$	$\pm 0.128$	$\pm 0.128$	$\pm 0.111$
NDE	0.271	0.254	0.223	0.066	0.067	<b>0.040</b>
	$\pm 0.169$	$\pm 0.103$	$\pm 0.140$	$\pm 0.074$	$\pm 0.076$	$\pm 0.067$
Avg. rank	5.363	5.272	4.090	2.545	2.363	<b>1.363</b>

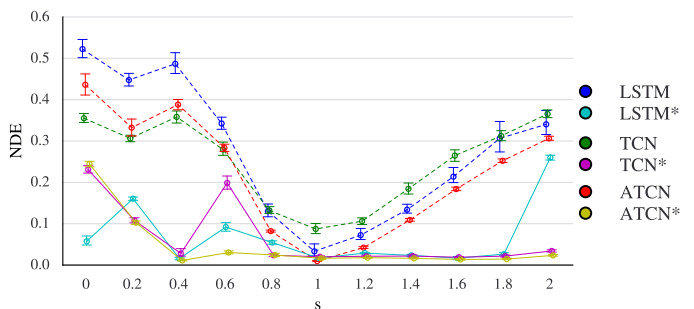


Fig. 4: NILM performance measured by NDE for DNN models trained on original and AMDA-augmented datasets (indicated by \*) and tested on artificially created test sets with varying scaling factors  $s$  applied to the BA appliance for the appliance variance scenario (see main text).

our previous experiment. To assess AMDA’s effectiveness, we analyze dataset size changes, performance improvements, and computational effort to highlight trade-offs between resource consumption and generalization capabilities.

Initially, we train the model using only the Office Offenbach dataset, referred to as **Base**, containing 631,152 data points, to set a performance baseline without any data augmentation. Next, we augment the training data by including the Dealer Offenbach configuration, resulting in the **Enlarged** dataset with 1,262,304 data points (a 100% increase relative to Base). This enlargement leads to improvements over the Base, with 14% reduction in MAE, 33% in MSE, 3% increase in  $R^2$ , and 32% reduction in NDE. The additional diversity in energy consumption patterns from the Dealer configuration likely contributes to these enhancements by providing a broader learning context for the model. The results are summarized in Table V and the NDE metric is graphically shown in Fig. 5.

As a comparative data augmentation method, we apply the **Random Data Augmentation (RDM)** approach [42]. This involves generating 14 scaled versions for each appliance’s signal, ranging from an 80% reduction to a 1000% increase in appliance power. The number of scaled versions is bounded to our computation limits and it has been selected arbitrarily, just for demonstration reasons. This results in a total of 12,623,040 data points (a 1900% increase relative to Base). Using this approach, we observe improvements of 18% in MAE, 37% in MSE, 123% in  $R^2$ , and 35% in NDE compared to Base

performance.

Finally, we apply AMDA (Algorithm 1) to both the Base and Enlarged datasets, resulting in the **Base\*** (1,893,456 data points, a 200% increase relative to Base) and **Enlarged\*** (2,524,608 data points, a 300% increase relative to Base) datasets. For each augmented dataset, we generate one additional re-scaled dataset using a randomly selected scaling factor  $s$  from the range  $[1, 5]$ . In each case, only one value of  $s$  is applied for data augmentation, ensuring moderate variability without distorting appliance behavior. The results reported here use  $s = 1.73$ , with other tested values giving similar results both qualitatively and quantitatively.

With AMDA, we achieve significant improvements. For the Base\* dataset, we observe improvements of 55% in MAE, 80% in MSE, 260% increase in  $R^2$ , and 72% reduction in NDE compared to Base performance. For the Enlarged\* dataset, the improvements are even more substantial: 86% in MAE, 97% in MSE, 340% increase in  $R^2$ , and 79% reduction in NDE compared to Base. These results demonstrate the effectiveness of AMDA in enhancing model generalization to different facilities.

These results are reported in Table V, along with training time and computational effort measured in GFLOPS (Giga Floating Point Operations per Second) as estimated by the `THOP: PyTorch-OpCounter` [43] function in `PyTorch` to show order of magnitude estimation of the computational effort. Both AMDA and RDM methods generate augmented samples via arbitrary controlled scaling factors (RDM uses 14 factors for demonstration purposes and computational boundaries). With the analysis reported in Table V, we highlight the informed modulation property of AMDA and the consequent efficiency. Despite RDM’s larger data volume, it does not yield better accuracy than AMDA. Specifically, using the proposed AMDA requires less training time compared to RDM while achieving better performance. For example, the Enlarged\* method takes approximately 22 hours to train, whereas the RDM method requires 74 hours. AMDA also demands fewer computational resources, with the Enlarged\* method utilizing 356 GFLOPS, significantly less than the 1,040 GFLOPS required by RDM. The training time and computational effort for AMDA are reduced by approximately 70% and 66%, respectively, compared to RDM. This demonstrates that AMDA provides a more efficient augmentation strategy, which is crucial for practical applications where computational resources and time are limited.

Additionally, we define the Maximum-achievable-Performance (MP) by training the model directly on the test configuration (Logistics, Los Angeles), serving as an upper bound in our analysis. The MP achieves a MAE of 0.021 MW, MSE of 0.001 MW<sup>2</sup>,  $R^2$  of 0.983, and NDE of 0.009, providing a benchmark to evaluate how close our methods approach optimal performance. For statistical robustness demonstration, we use the Friedman non-parametric test with a 0.05 confidence level, followed by the Nemenyi post-hoc test, and present the results in the Critical Difference plot [41] in Fig. 6. The plot indicates that the AMDA variants consistently outperform their counterparts in all scenarios tested, with **Enlarged\*** emerging as the

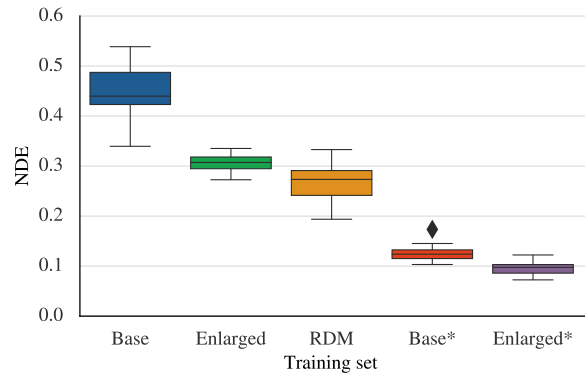


Fig. 5: NILM performance on the test dataset of a Logistics facility in Los Angeles with NDE metric in the Facility Variation Scenario for several training datasets: Base (Office Offenbach), Enlarged (Base + Dealer Offenbach), Random Data Augmentation (RDM), and AMDA-augmented datasets. Asterisks (\*) indicate datasets augmented with AMDA.

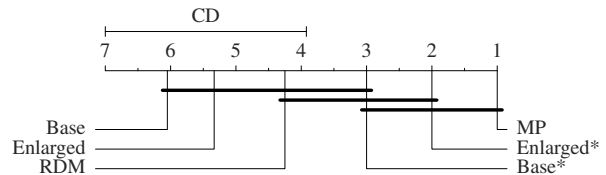


Fig. 6: Critical Difference diagram summarizing Experiment 2. Asterisks (\*) indicate datasets augmented with AMDA.

best performer. Notably, the methods with AMDA are not statistically different from the MP, indicating that our approach achieves performance close to the theoretical upper bound, while requiring only a marginal increase in training data and effort.

### C. Data Distribution Alignment Analysis

We project the time-series training signals of the **Base** dataset and its AMDA-augmented version **Base\*** onto a two-dimensional space using UMAP, as shown in Figure 7. Focusing on the CHP target appliance, we provide a zoomed section to emphasize the CHP-related data.

The left panel depicts the Base training data alongside the test CHP data from the Logistics Los Angeles building configuration. While there is some overlap between the training and test CHP data, a significant portion of the test data lies in regions where the training data is sparse, particularly in the lower right part of the plot. This indicates that models trained on the Base dataset may need to extrapolate in these regions, potentially reducing their accuracy.

In contrast, the right panel shows the AMDA-augmented **Base\*** data. The augmented data covers a larger region of the feature space and extends towards the complete range of the test CHP data. This suggests that AMDA effectively enriches the training data, preserving the structure and neighborhood relations of the data samples through relative scaling. As a result, models trained with AMDA-augmented data are better equipped to generalize to unseen data.

TABLE V: Average results of experiment ‘Facility Variation Scenario’. Datasets marked with (\*) are augmented using AMDA. The average rank is computed by ranking each method for each performance metric and averaging these ranks. We also report dataset sizes with relative increases compared to the Base, as well as Training Time and Computational Effort.

Dataset	Base	Enlarged	RDM	Base*	Enlarged*
Dataset Sample Size	631,152	1,262,304 (+100%)	12,623,040 (+1900%)	1,893,456 (+200%)	2,524,608 (+300%)
MAE [MW]	$0.155 \pm 0.007$	$0.132 \pm 0.005$	$0.127 \pm 0.012$	$0.080 \pm 0.006$	<b><math>0.069 \pm 0.006</math></b>
MSE [MW <sup>2</sup> ]	$0.048 \pm 0.005$	$0.032 \pm 0.002$	$0.030 \pm 0.004$	$0.013 \pm 0.002$	<b><math>0.010 \pm 0.001</math></b>
R <sup>2</sup>	$0.216 \pm 0.092$	$0.224 \pm 0.034$	$0.482 \pm 0.058$	$0.778 \pm 0.024$	<b><math>0.950 \pm 0.026</math></b>
NDE	$0.451 \pm 0.051$	$0.305 \pm 0.017$	$0.290 \pm 0.035$	$0.127 \pm 0.016$	<b><math>0.093 \pm 0.013</math></b>
Training Time [hrs]	5	10	74	17	22
Computational Effort [GFLOPS]	85	250	1,040	250	356
Avg. Rank	5.00	4.00	3.00	2.00	1.00

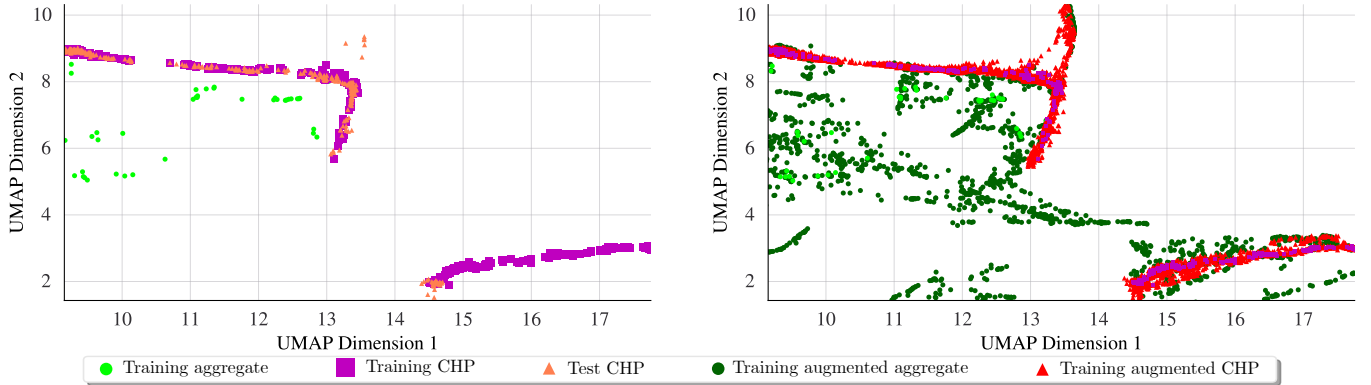


Fig. 7: Detail of two-dimensional UMAP projections of energy signals for the CHP appliance. Left: **Base** training data and target CHP data. Right: AMDA-augmented **Base\*** data and target CHP data.

TABLE VI: KL and JS divergence values between each training and the test dataset. Lower values indicate better alignment with the test distribution. Percentages show a reduction compared to the Base dataset.

Dataset	KL Div.	% Red.	JS Div.	% Red.
Base	0.645	-	0.350	-
Enlarged	0.553	14%	0.326	7%
RDM	0.518	20%	0.297	15%
Base* (AMDA)	0.335	48%	0.224	36%
Enlarged* (AMDA)	<b>0.314</b>	<b>51%</b>	<b>0.180</b>	<b>49%</b>

To quantitatively analyze the alignment between the distributions of the CHP data in different training datasets, we compute the KL divergence and JS divergence between each training dataset and the test set, calculated from the original data distributions (not from the UMAP projections), as reported in Table VI. We observe that the AMDA-augmented datasets (Base\* and Enlarged\*) have significantly lower KL and JS divergence values compared to the other methods. Specifically, the KL divergence for Enlarged\* is 0.314, a reduction of approximately 51% compared to the Base dataset (0.645). The JS divergence for Enlarged\* is 0.180, representing a reduction of about 49% compared to the Base dataset (0.350). This improved alignment is crucial for the model’s ability to generalize to unseen data, leading to better performance in energy disaggregation tasks.

## VII. CONCLUSIONS AND FUTURE WORK

We addressed the central challenge of data scarcity in purely data-driven industrial Non-Intrusive Load Monitoring (NILM) approaches, by introducing the Synthetic Industrial Dataset for Energy Disaggregation (SIDED). SIDED is a high-quality dataset of electricity consumption and production profiles for industrial facilities, generated using a Digital Twin. It encompasses three different types of facilities across three geographic locations, providing diverse scenarios for NILM research. The configuration possibilities in industrial facilities, due to the variety in types and sizes of appliances, are much greater than in typical household settings. Consequently, generating datasets that cover a wide range of possible configurations is often not feasible, which hinders the generalization capabilities of machine learning-based NILM models. To address this, we also introduced the Appliance-Modulated Data Augmentation (AMDA) method, which generates a large amount of training data with increased variability by scaling appliance contributions based on their relative impact in a simple and computationally efficient manner. Our experiments demonstrated that AMDA enhances the generalization and generalization of NILM models in industrial settings using the SIDED dataset. Models trained with AMDA effectively disaggregated signals even when primary appliances were scaled to out-of-distribution sizes in the test data, simulating changes in appliance behavior. Additionally, we assessed the generalization capabilities of NILM models trained with AMDA on unseen building configurations.

The results showed that augmenting the training data with AMDA led to significant performance improvements, surpassing those achieved with conventional data augmentation methods.

While SIDED provides a valuable resource for industrial NILM research, it has limitations. Factors such as unlabeled appliance data and measurement noise present in actual facilities might not be fully represented. Regarding the AMDA method, its effectiveness relies on the assumption that scaling appliance contributions based on their relative impact can capture the variability seen in different industrial scenarios. However, AMDA assumes that the scaling of appliances does not lead to unrealistic operational states given specific domain knowledge. Therefore, care must be taken to ensure that the augmented data remains within realistic bounds.

Expanding SIDED with additional configurations and appliance types can further enhance its utility. Integrating the SIDED dataset and AMDA into online learning scenarios or federated learning settings with non-IID data [44] and constrained resources environment [45], can be explored.

#### ACKNOWLEDGMENT

Christian Internò acknowledges funding from the Honda Research Institute Europe.

#### REFERENCES

- [1] International Energy Agency, *World Energy Outlook 2021*. Paris: IEA Publications, 2021. [Online]. Available: <https://www.iea.org/reports/world-energy-outlook-2021>
- [2] S. Darby, "The effectiveness of feedback on energy consumption," *A Review for DEFRA of the Literature on Metering, Billing and direct Displays*, vol. 486, 01 2006.
- [3] J. Engel, T. Schmitt, T. Rodemann, and J. Adamy, "Hierarchical MPC for building energy management: Incorporating data-driven error compensation and mitigating information asymmetry," *Applied Energy*, 2024.
- [4] P. A. Schirmer and I. Mporas, "Non-intrusive load monitoring: A review," *IEEE Transactions on Smart Grid*, vol. 14, no. 1, pp. 769–784, 2023.
- [5] D. Renaux, R. Linhares, F. Pottker, A. Lazzaretti, C. Lima, A. Coelho Neto, and M. Campaner, "Designing a novel dataset for non-intrusive load monitoring," in *2018 VIII Brazilian Symposium on Computing Systems Engineering (SBESC)*, 2018, pp. 243–249.
- [6] A. Castellani, S. Schmitt, and B. Hammer, "Estimating the electrical power output of industrial devices with end-to-end time-series classification in the presence of label noise," *CoRR*, vol. abs/2105.00349, 2021.
- [7] A. Verma, A. Anwar, M. A. P. Mahmud, M. Ahmed, and A. Kouzani, "A comprehensive review on the nilm algorithms for energy disaggregation," 2021.
- [8] M. D'Incecco, S. Squartini, and M. Zhong, "Transfer learning for non-intrusive load monitoring," *IEEE Transactions on Smart Grid*, vol. 11, no. 2, pp. 1419–1429, 2020.
- [9] H. K. Iqbal, F. H. Malik, A. Muhammad, M. A. Qureshi, M. N. Abbasi, and A. R. Chishti, "A critical review of state-of-the-art non-intrusive load monitoring datasets," *Electric Power Systems Research*, vol. 192, p. 106921, 2021.
- [10] F. Kalinke, P. Bielski, S. Singh, E. Fouché, and K. Böhm, "An evaluation of nilm approaches on industrial energy-consumption data," in *Proceedings of the Twelfth ACM International Conference on Future Energy Systems*, ser. e-Energy '21. New York, NY, USA: Association for Computing Machinery, 2021, p. 239–243.
- [11] Y. Yan, L. Zhu, A. Yang, Y. Zhi, B. Liu, Y. Huang, and H. Wen, "A review of industrial non-intrusive load monitoring," in *2023 International Conference on Sensing, Measurement & Data Analytics in the era of Artificial Intelligence (ICSMD)*. IEEE, 2023, pp. 1–6.
- [12] G.-F. Angelis, C. Timplalexis, S. Krinidis, D. Ioannidis, and D. Tzovaras, "Nilm applications: Literature review of learning approaches, recent developments and challenges," *Energy and Buildings*, vol. 261, p. 111951, 2022.
- [13] H. Yin, K. Zhou, and S. Yang, "Non-intrusive load monitoring by load trajectory and multi feature based on dcnn," *IEEE Transactions on Industrial Informatics*, pp. 1–12, 2023.
- [14] S. Kurma, K. Singh, M. Katwe, S. Mumtaz, and C.-P. Li, "Risk-empowered mec for urlc systems with digital-twin-driven architecture," in *IEEE INFOCOM 2023 - IEEE Conference on Computer Communications Workshops (INFOCOM WKSHPS)*, 2023, pp. 1–6.
- [15] A. Castellani, S. Schmitt, and S. Squartini, "Real-world anomaly detection by using digital twin systems and weakly supervised learning," *IEEE Transactions on Industrial Informatics*, vol. 17, no. 7, pp. 4733–4742, 2021.
- [16] W. Yu, P. Patros, B. Young, E. Klinac, and T. G. Walmsley, "Energy digital twin technology for industrial energy management: Classification, challenges and future," *Renewable and Sustainable Energy Reviews*, vol. 161, p. 112407, 2022.
- [17] J. Donnal, "Nilm-synth: Synthetic dataset generation for non-intrusive load monitoring algorithms," in *2022 IEEE Power & Energy Society Innovative Smart Grid Technologies Conference (ISGT)*, 2022, pp. 1–6.
- [18] T. Schwan, S. Schmitt, and A. Castellani, "Calibration of HVAC system models with monitoring data - Digital Twin meets measurement data," in *ESI FORUM IN DEUTSCHLAND*. ESI, 2019. [Online]. Available: <https://www.honda-ri.de/publications/publications/?pubid=4160>
- [19] G. Iglesias, E. Talavera, Á. González-Prieto, A. Mozo, and S. Gómez-Canaval, "Data augmentation techniques in time series domain: a survey and taxonomy," *Neural Computing and Applications*, vol. 35, no. 14, pp. 10 123–10 145, 2023.
- [20] I. Abubakar, S. N. Khalid, M. W. Mustafa, H. Shareef, and M. Mustapha, "An overview of non-intrusive load monitoring methodologies," in *2015 IEEE Conference on Energy Conversion (CENCON)*, 2015, pp. 54–59.
- [21] A. Harell, R. Jones, S. Makonin, and I. V. Bajić, "Tracegan: Synthesizing appliance power signatures using generative adversarial networks," *IEEE Transactions on Smart Grid*, vol. 12, no. 5, pp. 4553–4563, 2021.
- [22] W. Kong, Z. Y. Dong, B. Wang, J. Zhao, and J. Huang, "A practical solution for non-intrusive type ii load monitoring based on deep learning and post-processing," *IEEE Transactions on Smart Grid*, vol. 11, no. 1, pp. 148–160, 2020.
- [23] Y. Tao, J. Qiu, S. Lai, X. Sun, Y. Ma, and J. Zhao, "Customer-centered pricing strategy based on privacy-preserving load disaggregation," *IEEE Transactions on Smart Grid*, vol. 14, no. 5, pp. 3401–3412, 2023.
- [24] A. S. Cespedes-Cubides and M. Jradi, "A review of building digital twins to improve energy efficiency in the building operational stage," *Energy Informatics*, vol. 7, no. 1, p. 11, 2024. [Online]. Available: <https://doi.org/10.1186/s42162-024-00313-7>
- [25] P. Bandeira de Mello Martins, V. Barbosa Nascimento, A. R. de Freitas, P. Bittencourt e Silva, and R. Guimarães Duarte Pinto, "Industrial machines dataset for electrical load disaggregation," 2018.
- [26] M. Ehrmann, M. Romanello, S. Clematide, and A. Doucet, "Introducing the HIPE 2022 Shared Task: Named Entity Recognition and Linking in Multilingual Historical Documents," in *Proceedings of the 44<sup>th</sup> European Conference on IR Research (ECIR 2022)*. Stavanger, Norway: Lecture Notes in Computer Science, Springer, 2022. [Online]. Available: [https://link.springer.com/chapter/10.1007/978-3-030-99739-7\\_44](https://link.springer.com/chapter/10.1007/978-3-030-99739-7_44)
- [27] M. Kahl, V. Krause, R. Hackenberg, A. Haq, A. Horn, H.-a. Jacobsen, T. Kriechbaumer, M. Petzenhauser, M. Shamonin, and A. Udalzow, "Measurement system and dataset for in-depth analysis of appliance energy consumption in industrial environment," *tm - Technisches Messen*, vol. 86, 10 2018.
- [28] G. Tanoni, E. Principi, and S. Squartini, "Non-intrusive load monitoring in industrial settings: A systematic review," *Renewable and Sustainable Energy Reviews*, vol. 202, p. 114703, 2024. [Online]. Available: <https://www.sciencedirect.com/science/article/pii/S1364032124004295>
- [29] Y. Yan, L. Zhu, A. Yang, Y. Zhi, B. Liu, Y. Huang, and H. Wen, "A review of industrial non-intrusive load monitoring," in *2023 International Conference on Sensing, Measurement & Data Analytics in the era of Artificial Intelligence (ICSMD)*, 2023, pp. 1–6.
- [30] C. Li, K. Zheng, H. Guo, and Q. Chen, "A mixed-integer programming approach for industrial non-intrusive load monitoring," *Applied Energy*, vol. 330, p. 120295, 2023. [Online]. Available: <https://www.sciencedirect.com/science/article/pii/S0306261922015525>
- [31] A. Yaniv and Y. Beck, "Advances in non-intrusive load monitoring for the industrial domain: Challenges, insights, and path forward," *Renewable and Sustainable Energy Reviews*, vol. 210, p. 115136, 2025. [Online]. Available: <https://www.sciencedirect.com/science/article/pii/S1364032124008621>
- [32] N. Batra, J. Kelly, O. Parson, H. Dutta, W. Knottenbelt, A. Rogers, A. Singh, and M. Srivastava, "NILMTK," in *Proceedings of the 5th international conference on Future energy systems*. ACM, jun 2014.

- [33] J. Engel, A. Castellani, P. Wollstadt, F. Lanfermann, T. Schmitt, S. Schmitt, L. Fischer, S. Limmer, D. Luttrupp, F. Jomrich, R. Unger, and T. Rodemann, "A real-world energy management data set from a smart company building for optimization and machine learning," *DRYAD*, 2025. [Online]. Available: <https://doi.org/10.5061/dryad.73n5tb363>
- [34] —, "A real-world energy management dataset from a smart company building for optimization and machine learning," *arXiv.2503.11469*, 2025. [Online]. Available: <https://doi.org/10.48550/arXiv.2503.11469>
- [35] S. Naderian, "Machine learning approach for non-intrusive load monitoring in smart grids: new deep learning method based on long short-term memory and convolutional neural networks," in *2022 8th Iranian Conference on Signal Processing and Intelligent Systems (ICSPIS)*, 2022, pp. 1–7.
- [36] G. Liu, G. Liang, H. Zhao, J. Zhao, J. Liu, and Z. Wu, "A temporal convolutional neural network with attention mechanism for industrial non-intrusive load monitoring," in *2021 IEEE 5th Conference on Energy Internet and Energy System Integration (EI2)*, 2021, pp. 3279–3284.
- [37] C. Zhang, M. Zhong, Z. Wang, N. Goddard, and C. Sutton, "Sequence-to-point learning with neural networks for non-intrusive load monitoring," in *Proceedings of the Thirty-Second AAAI Conference on Artificial Intelligence and Thirtieth Innovative Applications of Artificial Intelligence Conference and Eighth AAAI Symposium on Educational Advances in Artificial Intelligence*, ser. AAAI'18/IAAI'18/EAAI'18. AAAI Press, 2018.
- [38] F. Pedregosa, G. Varoquaux, A. Gramfort, V. Michel, B. Thirion, O. Grisel, M. Blondel, P. Prettenhofer, R. Weiss, V. Dubourg, J. Vanderplas, A. Passos, D. Cournapeau, M. Brucher, M. Perrot, and E. Duchesnay, "Scikit-learn: Machine learning in Python," *Journal of Machine Learning Research*, vol. 12, pp. 2825–2830.
- [39] C. Klemenjak, S. Makonin, and W. Elmenreich, "Towards comparability in non-intrusive load monitoring: On data and performance evaluation," in *2020 IEEE Power & Energy Society Innovative Smart Grid Technologies Conference (ISGT)*, 2020, pp. 1–5.
- [40] L. McInnes and J. Healy, "Umap: Uniform manifold approximation and projection for dimension reduction," *arxiv:802.03426*, 2018.
- [41] J. Demšar, "Statistical comparisons of classifiers over multiple data sets," *Journal of Machine Learning Research*, vol. 7, no. 1, pp. 1–30, 2006.
- [42] A. Delfosse, G. Hébrail, and A. Zerroug, "Deep learning applied to nilm: Is data augmentation worth for energy disaggregation?" in *European Conference on Artificial Intelligence*, 2020.
- [43] L. Zhu, "Thop: Pytorch-opcounter," *THOP: PyTorch-OpCounter*, 2022.
- [44] C. Internò, M. Olhofer, Y. Jin, and B. Hammer, "Federated loss exploration for improved convergence on non-iid data," in *2024 International Joint Conference on Neural Networks (IJCNN)*, 2024, pp. 1–8.
- [45] C. Internò, E. Raponi, N. van Stein, T. Bäck, M. Olhofer, Y. Jin, and B. Hammer, "Adaptive hybrid model pruning in federated learning through loss exploration," in *International Workshop on Federated Foundation Models in Conjunction with NeurIPS 2024*, 2024. [Online]. Available: <https://openreview.net/forum?id=OxpWu6J0TW>